Optimal Power Dispatch of Renewable and Non-Renewable Generation through a Second-Order Conic Model

Lucas do Carmo Yamaguti
Department of Electrical Engineering
São Paulo State University
Ilha Solteira, Brazil
lucas.yamaguti@unesp.br

Juan M. Home-Ortiz
Department of Electrical Engineering
São Paulo State University
Ilha Solteira, Brazil
juan.home@unesp.br

Mahdi Pourakbari-Kasmaei
Department of Electrical Engineering and Automation, Aalto University
Espoo, Finland
mahdi.pourakbari@aalto.fi

Sérgio F. Santos
Portucalense Univ. Infante D. Henrique and INESC TEC
Porto, Portugal
sdfsantos@gmail.com

José Roberto Sanches Mantovani
Department of Electrical Engineering
São Paulo State University
Ilha Solteira, Brazil
mant@dee.feis.unesp

João P. S. Catalão
Faculty of Engineering of the University of Porto and INESC TEC
Porto, Portugal
catalao@fe.up.pt

2021 IEEE International Conference on Environment and Electrical Engineering and 2021 IEEE Industrial and Commercial Power Systems Europe (EEEIC / I&CPS Europe) | 978-1-6654-3613-7/21/$31.00 ©2021 IEEE | DOI: 10.1109/EEEIC/ICPSEurope51590.2021.9584817

***Abstract*—This work presents an extension of a second-order conic programming model (SOCP) to handle the multi-objective optimal power dispatch problem considering the probabilistic nature of some parameters related to power demand and the renewable energy sources (RES) generation, such as wind speed and solar irradiation level. Three objective functions are considered in this study: 1) costs of RES and non-RES generation; 2) active power losses in the transmission system; and, 3) emission pollutant gases produced by fossil fuel-based generating units. The stochastic nature of power demands and RES are developed through a set of representative operational scenarios extracted from historical data and via a scenario reduction technique. The results obtained in the SOCP model are compared with a nonlinear programming (NLP) model to check the robustness and precision of SOCP model. To this, both models are implemented and processed to simulate the optimal flow for the IEEE 57- and 118-bus systems.**

Keywords— Emission pollutant gases, multi-objective optimization, optimal power dispatch, renewable energy, second-order conic programming.

NOMENCLATURE

Indices and sets:

b	Index for time block;
t, h, w, ph	Index for thermoelectric, hydroelectric, wind, and photovoltaic generations;
k	Index for buses;
km	Index for branches;
D, ω, Ir	Index for level of demand, wind speed, and solar irradiation;
s	Index for stochastic scenarios;
Γ_B	Set of branches;
Γ_G	Set of generation buses;
Γ_N	Set of nodes;
Ω_b	Set of time blocks;
Ω_b^s	Set of scenarios in time block b;

Parameters:

b_k^{sh}, g_k^{sh}	Shunt susceptance/conductance in the bus;
b_{km}, g_{km}	Series susceptance/conductance in the branch;
b_{km}^{sh}, g_{km}^{sh}	Shunt susceptance/conductance in the branch;
c_2^t, c_1^t, c_0^t	Quadratic, linear, and constant cost coefficients of non-renewable generations;
$c_1^h, c_1^w, c_1^{ph}, c_0^h, c_0^w, c_0^{ph}$	Linear and constant cost coefficients of hydroelectric, wind, and photovoltaic generations;
c^{al}	Active power loss cost coefficient;
hr_b	Duration of the time blocks.
P_l^D, Q_l^D	Active and reactive power demand;
$\underline{P^t}, \underline{P^h}, \underline{P^w}, \underline{P^{ph}}, \underline{Q^t}, \underline{Q^h}$	Minimum limit of active/reactive power injected;
$\overline{P^t}, \overline{P^h}, \overline{P^w}, \overline{P^{ph}}, \overline{Q^t}, \overline{Q^h}$	Maximum limit of active/reactive power injected;
P_{Rw}^w, P_{RI}^{ph}	Nominal active power of the wind and photovoltaic generators;
S_{km}	Maximum apparent power flow through branch km;
S^t, S^h, S^w	Apparent power limit for thermoelectric, hydroelectric, and wind generators;
$tg(\delta^{w_{CAP}}), tg(\delta^{w_{IND}})$	Reactive power injection factors of wind generations;
$tg(\delta^{ph_{CAP}}), tg(\delta^{ph_{IND}})$	Reactive power injection factors of photovoltaic generations;
$\overline{V}, \underline{V}$,	Minimum/maximum voltage magnitude limits;
$\alpha^t, \beta^t, \gamma^t, \zeta^t, \lambda^t$	Emission coefficients for active power generation in thermal generators.;
a_{km}, φ_{km}	Voltage transformation and angular offset of the transformer;
π, ρ	Mean value and probability of random variables;
τ_r^{Ir}	Rated solar irradiation level;
$\tau_l^\omega, \tau_0^\omega, \tau_R^\omega$	Minimum, maximum, rated wind speed;
σ	Objective function weight;

Variables:

d_k	Auxiliary variables related with the nodal voltage in the conic model;
e_{km}, f_{km}	Auxiliary variables related to the voltage drop in the branch in the conic model;
p^t, p^h, p^w, p^{ph}	Active power injected by the thermoelectric, hydroelectric, wind, and photovoltaic generations, respectively;
p_{km}, q_{km}	Active and reactive power flow in the branch ij;
q^t, q^h, q^w, q^{ph}	Active power injected by the thermoelectric, hydroelectric, wind, and photovoltaic generations;
θ_{km}	Bus voltage angle;
Ψ	Objective function;

I. INTRODUCTION

The optimal power dispatch (OPD) is a complex and large-size constrained nonlinear programming (NLP) problem that aims to optimize the power generation of the

Lucas do Carmo Yamaguti, Juan M. Home-Ortiz, and José Roberto Sanches Mantovani acknowledge the support by the São Paulo Research Foundation (FAPESP) under grants 2019/01841-5 2019/23755-3 and 2015/21972-6, in part by the Coordination for the Improvement of Higher Education Personnel (CAPES) finance code 001, and in part by the Brazilian National Council for Scientific and Technological Development (CNPq) under Grant 304726/2020-6.

J.P.S. Catalão acknowledges the support by FEDER funds through COMPETE 2020 and by Portuguese funds through FCT, under POCI-01-0145-FEDER-029803 (02/SAICT/2017).

electrical power system (EPS) to satisfy the power demand while considering the system's physical and operational constraints [1]. The NLP model is difficult to solve through classical optimization techniques due to its multimodal nature and high mathematical complexity. In this regard, recently in the literature, several convexification techniques have been developed to obtain the optimal global solution for the OPD problem through algebraic manipulations in the objective function and constraints. The second-order conic programming (SOCP) models are one of the most prominent in this area. These approaches allow a good trade-off between computational effort and the accuracy of the results. Besides, a convex formulation for the OPD permits that this problem can be approached from different views to be adapted to the new challenges of the modern EPS control operation. However, these convexification techniques may not accurately represent the original nonlinear model, therefore feasibility problems in the power balance equations can occur [2].

Nowadays, the EPS generation matrix is in transformation, and the fossil generation sources are replaced by renewable energy sources (RES) to reduce greenhouse gas (GHG) emissions and preserve the environment. Consequently, the generation of electric energy that uses fossil fuels started to be accompanied by RES due to the policies of environmental protocols that were established among the major world economic powers aiming to guarantee, among other objectives, the reduction of greenhouse gas emissions [3], [4]. The inclusion of RES models in the EPS analysis increases the complexity of the problem due to uncertainties in the parameters that define the behavior of different types of RES [5]. In this way, stochastic approaches are more adequate to consider the uncertainty behaviors of RES and power demand, obtaining a more realistic, but complex model. On the other hand, GHG emission mitigation changes the single objective of OPD for a multi-objective problem, so new optimization models and procedures for analysis and planning of operation of the EPS must be developed.

In the literature, the OPD problem has been proposed to solve the economic and environmental dispatch, through probabilistic and metaheuristic approaches [6]–[10]. In [6], a multi-objective economic power dispatch model was proposed, where the objective function minimizes the cost of generation and the emission of pollutants from generation sources that use fossil fuels. The problem is modeled as an integer NLP problem and solved using an evolutionary algorithm that preserves the diversity of the population and provides an optimized Pareto front in small-size systems. In [7], the problem of optimal dispatch of active power was solved using the multi-objective differential evolution algorithm to minimize generation costs, losses of active power in the network, and emission of GHG. In [8], the problem of economic dispatch of thermoelectric generations (TG) in EPS was formulated through two models of fractional nonlinear programming to minimize the total cost of generation and greenhouse gas emissions from generating units that use fossil fuels. The solutions to the problem were determined by Dinkelbach's algorithm that converts a problem with the fractional objective function into a sequence of non-fractional minimization problems. In [9], the multi-objective probabilistic optimal power flow (OPF) model for the medium-term operation of EPS considering high penetration of RES was proposed. To deal with the nonlinearities of the model, an NSGA-II algorithm was used to solve the problem. The uncertainties of the RES parameters and the demands are incorporated through a fast and efficient point-estimate method probabilistic, while the operational state of the system was determined by the classical Newton AC power flow method. In [10], a probabilistic multi-objective OPF problem was used to minimize the generation cost and GHG emission. This approach considered the TG, hydroelectric generation (HG), and wind turbines. Uncertainties were taken into account with random variables of wind speed and demand levels. The solutions to the problem were determined by a biogeography-based optimization algorithm, while the analysis of uncertainty parameters was developed using the point estimate method.

In this paper, a SOCP multi-objective stochastic scenario-based model for the OPD problem with renewable (eolic, photovoltaic, and hydroelectric generations) and non-renewable (thermoelectric generation) energy sources is proposed. Three simultaneous objective functions are considered in the formulation: 1) costs of RES and non-RES generation; 2) active power losses in the transmission branches and 3) GHG emission mitigation. These objective functions are considered through the *a priori* decision method based on their weighting of the objective. A set of representative operational scenarios is generated from historical data using a scenario reduction technique over one year, (8760 h), to considering the uncertainty of RES in the period. Two cases of studies are performed through simulation with IEEE 57-, and 118-bus systems, considering some operating scenarios. The obtained results with the SOCP multi-objective model are compared with those of an equivalent multi-objective exact NLP model.

The main contributions of this paper are the following:

1. Proposal of a SOCP stochastic model for the OPD problem that includes renewable and non-renewable generation units.
2. Development of a multi-objective approach for the OPD problem with three objectives, where a sum weighted method is used to reformulate the multi-objective problem into a single objective optimization model.
3. Critical analysis of the convex model comparing the results obtained with the proposed SOCP multi-objective model with those from an equivalent NLP model. This analysis aims to verify the precision and validity of the solutions obtained with the convex model.

The remainder of this paper is organized as follows: Section II presents the modeling of the uncertainties and the formulations of the NLP and SOCP models for the OPD problem. In Section III, the results and discussion are presented. Finally, relevant conclusions are drawn in Section IV.

II. MATHEMATICAL MODELS

The uncertainties of variables and parameters that describe the EPS behavior have a significant impact on operational costs of the network. To handle this issue, a stochastic scenario-based approach is considered. In this paper, a SOCP multi-objective model is used to find the global optimization of the problem, and the weighted objectives are used to find its Pareto front.

A. Modeling uncertainty

The equations representing the operation of the system are modeled by a set of representative stochastic scenarios Ω derived from measurements of energy demand and RES, to guarantee an adequate representation of the uncertainties in the behavior of these parameters. In this approach, the considered horizon planning (8760h) is divided into b time blocks, as presented in Fig. 1, to duly represent seasonal characteristics and weather effects. To reduce the computational complexity, in each time block b in Ω_b, the load behavior, wind speed, and solar irradiation are represented through a set of scenarios using the duration curves methodology presented in [11]. This methodology uses cumulative distribution functions to determine different levels and probabilities of load behavior, wind speed, and solar irradiation. In this way, it is possible to describe scenarios in each block of time for each variable using pairs of information of average value and probability. Therefore, the sets of scenarios in each time block b for the level of demand, wind speed, and solar radiation is obtained according to $\Omega_b^D = (\pi_b^D, \rho_b^D), \Omega_b^\omega = (\pi_b^\omega, \rho_b^\omega), \Omega_b^{Ir} = (\pi_b^{Ir}, \rho_b^{Ir})$, respectively.

Fig. 2 shows the load curves, wind speed, and solar radiation and their respective pairs of (π, ρ) in each time block b. Fig. 1 shows the correlating of scenarios. A one-by-one combination of scenarios contained in the same block of time is carryout as follows: $\Omega_b^s = (\Omega_b^D, \Omega_b^\omega, \Omega_b^{Ir})\ \forall (b \in \Omega_b)$. The probability of each scenario is determined by the product of individual probabilities of each variable arranged in the same block of time, according to $\rho_b = \rho_b^D \rho_b^\omega \rho_b^{Ir}$ .For simplicity, it is assumed that all locations of the RES are subject to the same weather and seasonal conditions. Similarly, it is considered that all load buses are subject to the same variability.

B. Renewable energy sources modeling

The power produced by the wind generators (WG) is described in (1) as a piecewise formulation according to [12], [13]. The power produced by the photovoltaic (PV) generation is calculated according to (2) [13].

$$p^w(\tau^\omega) = \begin{cases} 0, & \tau^\omega < \tau_I^\omega \\ \frac{P_{Rw}^w}{\tau_R^\omega - \tau_I^\omega}\tau^\omega + P_{Rw}^w\left(1 - \frac{\tau_R^\omega}{\tau_R^\omega - \tau_I^\omega}\right), & \tau_I^\omega \le \tau^\omega < \tau_R^\omega \\ P_{Rw}^w, & \tau_R^\omega \le \tau^\omega < \tau_0^\omega \\ 0, & \tau^\omega \ge \tau_0^\omega \end{cases} \quad (1)$$

$$p^{ph}(\tau^{Ir}) = \begin{cases} P_{RI}^{ph}\frac{\tau^{Ir}}{\tau_r^{Ir}}, & 0 \le \tau^{Ir} \le \tau_r^{Ir} \\ P_{RI}^{ph}, & \tau^{Ir} \ge \pi_r^{Ir} \end{cases} \quad (2)$$

C. Optimal power dispatch model

The OPD problem is formulated through a multi-objective stochastic scenario-based nonlinear programming optimization model (3)–(26). In this formulation, three

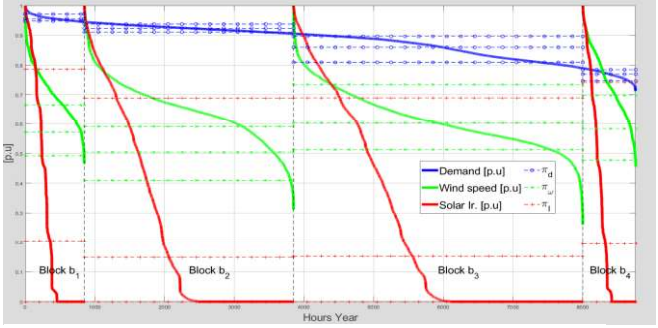

Fig. 2 - Demand, Wind speed, and Solar Ir. duration curves

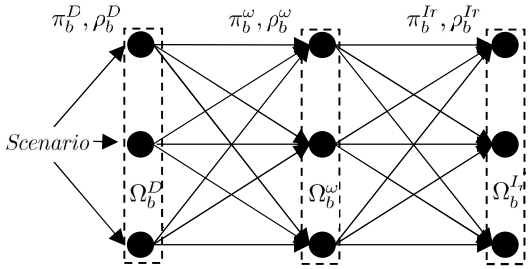

Fig. 1 - Combined stochastic scenarios in time block b

objectives are considered (3)–(5) [9]. In (3), the function F_1 determines the energy generation cost considering that are in operation on the system RES (HG, WG, and PV) modeled as a linear function, and non-RES (TG) modeled as a quadratic function. In (4), the function F_2 determines the cost of active power losses considering an active power loss cost coefficient, c^{al}. Finally, in (5) the function F_3 determines the emission of polluting gases (carbon, nitrogen and sulfur) in the environment by TGs [6]. In this formulation, the emission of polluting gases by RES is not considered.

$$F_1 = \sum_{t,h,w,ph \in \Gamma_G} \left(\left(\left(p_{b,s}^t\right)^2 c_2^t + p_{b,s}^t c_1^t + c_0^t\right) + \left(p_{b,s}^h c_1^h + c_0^h\right) + \left(p_{b,s}^w c_1^w + c_0^w\right) + \left(p_{b,s}^{ph} c_1^{ph} + c_0^{ph}\right)\right) \quad \begin{matrix} b \in \Omega_b; \\ s \in \Omega_b^s; \end{matrix} \quad (3)$$

$$F_2 = \left[\sum_{km \in \Gamma_B}\left(p_{km,b,s} + p_{mk,b,s}\right)\right] c^{al} \quad \begin{matrix} b \in \Omega_b; \\ s \in \Omega_b^s; \end{matrix} \quad (4)$$

$$F_3 = \sum_{t \in \Gamma_G}\left[10^{-2}\left(\alpha^t + \beta^t p_{b,s}^t + \gamma^t\left(p_{b,s}^t\right)^2\right) + \zeta^t e^{(\lambda^t p_{b,s}^t)}\right] \quad \begin{matrix} b \in \Omega_b; \\ s \in \Omega_b^s; \end{matrix} \quad (5)$$

In the objective function Ψ, presented in (6), the functions F_1, F_2, and F_3 are considered through the *a priori* decision method of weighting the objective functions, i.e., the objective functions are weighted by the positive parameters σ_1, σ_2, and σ_3 respectively. These weight parameters represent a convex combination since $\sigma_1 + \sigma_2 + \sigma_3 = 1$.

$$min: \Psi = \sum_{b \in \Omega_b}\left[(F_1\sigma_1 + F_2\sigma_2 + F_3\sigma_3) hr_b\ \rho_b\right] \quad (6)$$

The physical and operational conditions of EPS are determined through the set of restrictions (7)–(26).

$$\sum_{t,h,w,ph \in \Gamma_G}\left(p_{k,b,s}^t + p_{k,b,s}^h + p_{k,b,s}^w + p_{k,b,s}^{ph}\right) - P_{k,b,s}^D - \sum_{km \in \Gamma_B}\left(p_{km,b,s} + p_{mk,b,s}\right) - d_{k,b,s} g_k^{sh} = 0; \quad \begin{matrix} k \in \Gamma_N; \\ b \in \Omega_b; \\ s \in \Omega_b^s; \end{matrix} \quad (7)$$

$$\sum_{t,h,w,ph \in \Gamma_G}\left(q_{k,b,s}^t + q_{k,b,s}^h + q_{k,b,s}^w + q_{k,b,s}^{ph}\right) - Q_{k,b,s}^D - \sum_{km \in \Gamma_B}\left(q_{km,b,s} + q_{mk,b,s}\right) + d_{k,b,s} b_k^{sh} = 0; \quad \begin{matrix} k \in \Gamma_N; \\ b \in \Omega_b; \\ s \in \Omega_b^s; \end{matrix} \quad (8)$$

$$p_{km,b,s} = \left(a_{km} e^{j\varphi_{km}}\right)^2 d_{k,b,s} g_{km} - a_{km} e^{j\varphi_{km}}\left(g_{km} e_{km,b,s} + b_{km} f_{km,b,s}\right); \quad \begin{matrix} km \in \Gamma_B; \\ b \in \Omega_b; \\ s \in \Omega_b^s; \end{matrix} \quad (9)$$

$$p_{mk,b,s} = d_{m,b,s} g_{km} - a_{km} e^{j\varphi_{km}}\left(g_{km} e_{mk,b,s} - b_{km} f_{mk,b,s}\right); \quad \begin{matrix} mk \in \Gamma_B; \\ b \in \Omega_b; \\ s \in \Omega_b^s; \end{matrix} \quad (10)$$

$$q_{km,b,s} = -\left(a_{km} e^{j\varphi_{km}}\right)^2 d_{k,b,s}\left(b_{km} + b_{km}^{sh}/2\right) + a_{km} e^{j\varphi_{km}}\left(b_{km} e_{km,b,s} - g_{km} f_{km,b,s}\right); \quad \begin{matrix} km \in \Gamma_B; \\ b \in \Omega_b; \\ s \in \Omega_b^s; \end{matrix} \quad (11)$$

$$q_{mk,b,s} = -d_{m,b,s}\left(b_{km} + b_{km}^{sh}/2\right) + a_{km} e^{j\varphi_{km}}\left(b_{km} e_{mk,b,s} + g_{km} f_{mk,b,s}\right); \quad \begin{matrix} mk \in \Gamma_B; \\ b \in \Omega_b; \\ s \in \Omega_b^s; \end{matrix} \quad (12)$$

$$\underline{P^t} \le p_{b,s}^t \le \overline{P^t}; \qquad \underline{Q^t} \le q_{b,s}^t \le \overline{Q^t}; \quad \begin{matrix} t \in \Gamma_G; \\ b \in \Omega_b; \\ s \in \Omega_b^s; \end{matrix} \quad (13)$$

$$\left(p_{b,s}^t\right)^2 + \left(q_{b,s}^t\right)^2 \le \left(S^t\right)^2; \quad \begin{matrix} t \in \Gamma_G; \\ b \in \Omega_b; \\ s \in \Omega_b^s; \end{matrix} \quad (14)$$

$$\underline{P^h} \le p_{b,s}^h \le \overline{P^h}; \qquad \underline{Q^h} \le q_{b,s}^t \le \overline{Q^h}; \quad \begin{matrix} h \in \Gamma_G; \\ b \in \Omega_b; \\ s \in \Omega_b^s; \end{matrix} \quad (15)$$

$$\left(p_{b,s}^h\right)^2 + \left(q_{b,s}^t\right)^2 \le \left(S^h\right)^2; \quad \begin{matrix} h \in \Gamma_G; \\ b \in \Omega_b; \\ s \in \Omega_b^s; \end{matrix} \quad (16)$$

$$0 \le p_{b,s}^{w} \le \overline{P^{w}}\ ; \quad \begin{matrix} w \in \Gamma_G; \\ b \in \Omega_b; \\ s \in \Omega_b^s; \end{matrix} \tag{17}$$

$$-p_{b,s}^{w} tg(\delta^{w_{CAP}}) \le q_{b,s}^{w} \le p_{b,s}^{w} tg(\delta^{w_{IND}})\ ; \quad \begin{matrix} w \in \Gamma_G; \\ b \in \Omega_b; \\ s \in \Omega_b^s; \end{matrix} \tag{18}$$

$$\left(p_{b,s}^{w}\right)^2 + \left(q_{b,s}^{w}\right)^2 \le (S^{w})^2\ ; \quad \begin{matrix} w \in \Gamma_G; \\ b \in \Omega_b; \\ s \in \Omega_b^s; \end{matrix} \tag{19}$$

$$0 \le p_{b,s}^{ph} \le \overline{P^{ph}}\ ; \quad \begin{matrix} ph \in \Gamma_G; \\ b \in \Omega_b; \\ s \in \Omega_b^s \end{matrix} \tag{20}$$

$$-p_{b,s}^{ph} tg(\delta^{ph_{CAP}}) \le q_{b,s}^{ph} \le p_{b,s}^{ph} tg(\delta^{ph_{IND}})\ ; \quad \begin{matrix} ph \in \Gamma_G; \\ b \in \Omega_b; \\ s \in \Omega_b^s\ ; \end{matrix} \tag{21}$$

$$p_{k,b,s}^{i} = \sum_{\substack{t \in \Gamma_G \\ k=i}} \left(p_{b,s}^{i}\right); \quad q_{k,b,s}^{i} = \sum_{\substack{t \in \Gamma_G \\ k=i}} \left(q_{b,s}^{i}\right); \quad \begin{matrix} i \in \Gamma_G; \\ k \in \Gamma_N; \\ b \in \Omega_b; \\ s \in \Omega_b^s; \end{matrix} \tag{22}$$

$$\underline{V_k^2} \le d_{k,b,s} \le \overline{V_k^2}\ ; \quad \begin{matrix} km \in \Gamma_B; \\ b \in \Omega_b; \\ s \in \Omega_b^s; \end{matrix} \tag{23}$$

$$-\pi/2 \le \theta_{k,b,s} - \theta_{m,k,s} \le \pi/2\ ; \quad \begin{matrix} km \in \Gamma_B; \\ b \in \Omega_b; \\ s \in \Omega_b^s; \end{matrix} \tag{24}$$

$$d_{m,b,s} = \left(a_{km} e^{j\varphi_{km}}\right)^2 d_{k,b,s}\ ; \quad \begin{matrix} km \in \Gamma_B; \\ b \in \Omega_b; \\ s \in \Omega_b^s; \end{matrix} \tag{25}$$

$$d_{k,b,s} d_{m,b,s} = \left(e_{km,b,s}\right)^2 + \left(f_{km,b,s}\right)^2\ ; \quad \begin{matrix} km \in \Gamma_B; \\ b \in \Omega_b; \\ s \in \Omega_b^s; \end{matrix} \tag{26}$$

The physical and operational constraints of the problem are represented for each time block of time, b, and operating scenario, s. Equations (7) and (8) represent the active and reactive power balances, respectively. Constraints (9)–(12) represent the active and reactive power flows through the system lines, respectively. Constraints (13)–(21) represent the power generation limits for TG, HG, WG, and PV units, respectively. Constraint (22) represents the active and reactive powers provided by RES and non-RES in the generating bars and considering the presence of multi-generators in each bar. The voltage limits and angular opening limits of transmission lines are represented in constraints (23) and (24). Constraint (25) determines the transformation ratio and voltage magnitudes of the transformers with tap controls. Finally, in equation (26), the conic voltage restriction is defined using the auxiliary variables of the module (d), and real-imaginary voltage components (e, f).

Formulation (3)-(26) can be represented as a convex equivalent model of SOCP relaxing the conic voltage relation (26), as presented in (27). All other constraints of the SOCP model are the same as the NLP programming model (3)-(25).

$$d_{k,b,s} d_{m,b,s} \ge \left(e_{km,b,s}\right)^2 + \left(f_{km,b,s}\right)^2; \quad \begin{matrix} km \in \Gamma_B; \\ b \in \Omega_b; \\ s \in \Omega_b^s; \end{matrix} \tag{27}$$

III. TESTS AND RESULTS

The proposed NLP and SOCP models to solve the OPD problem considering RES and non-RES are programmed in AMPL [14]. The NLP model (3)–(26) is solved using KNITRO and the SOCP model (3)–(25), (27) is solved using CPLEX. The IEEE 57- and 118-bus system simulated in this work are available in the PGLib-OPF v19.05 [15]. The adopted costs for generations can be found in [6], [9], [15], [16]. Of note, during the simulations, minimum resistance equal to 10^{-4} [p.u] was adopted for branches where the resistance is zero for a more accurate SOCP model [17], [18]. Numerical experiments were processed on a server with an Intel Xeon processor, 2.2 GHz, and 64 GB of RAM.

TABLE I
Wind and solar irradiation levels

hr_b	π_b^{ω} (m/s)	ρ_b^{ω}	π_b^{Ir} (W/m^2)	ρ_b^{Ir}	T_{amb_b}(°C)
b_1 (850)	9.9728	0.30	860.8997	0.3000	32.9691
	8.5662	0.40	224.4728	0.2376	28.3823
	7.3690	0.30	0.0000	0.4624	23.4981
b_2 (3000)	8.8486	0.30	754.3633	0.3000	32.6124
	7.5551	0.40	162.6225	0.2417	27.8632
	6.1259	0.30	0.0000	0.4583	23.3531
b_3 (4150)	10.9971	0.30	755.4192	0.3000	30.9607
	9.0462	0.40	165.9477	0.2414	25.8010
	7.6863	0.30	0.0000	0.4586	21.2029
b_4 (760)	10.4605	0.30	812.4897	0.3000	32.8750
	8.7318	0.40	213.2312	0.2474	28.2776
	7.1472	0.30	0.0000	0.4526	23.2798

In the simulations, two case studies with different sources of generations were considered as follows:

- **Case E1 –** only TG generation is considered.
- **Case E2 –** all the generation technologies are considered (TG, HG, WG, and PV).

In Case E2, the wind turbines, VESTAS v80 2 MW, and the photovoltaic panels GCL-P6/72 330 were used. RESs replaced some non-RES units installed in the EPS and were dimensioned to provide a maximum total power of 1 GW. The c^{al} used was 120 US$/MWh [19]. The uncertainty in the behavior of the electrical demand of the system was determined using a normal distribution.

For all case studies, historical data on the behavior of wind speed and solar radiation were obtained from [20] over one year, (8760 h), for the Northeast region of Brazilian. In this work, the uncertainty of wind speed, and solar irradiation was modeled into 04 blocks of time, and the demand in 03 levels (light, nominal and heavy), resulting in 108 scenario analyses. The levels of wind speed and solar radiation used in simulations are shown in TABLE I. Previous experiments showed that these scenarios satisfactorily describe the operational behavior of the analyzed systems during one year. For both cases, to obtain the Pareto front, the weight parameters σ in the objective function Ψ take values in steps of 0.1, considering all possible convex combinations.

A. IEEE 57-bus system

The IEEE 57-bus system is small-sized and has relative computational difficulty. TABLE II presents the average levels and the probabilities of the demand scenarios. For Case E1, all the generation units are TG. For Case E2, buses 8 and 12 are HG units, buses 1 and 2 are WT, buses 6 and 9 are PV, and the remainder of the generation units are TG.

TABLE III and TABLE IV present the solution giving by NLP and SOCP models, highlighting the extreme points of the obtained Pareto front and the lower value of the objective function Ψ for Cases E1 and E2, respectively. The results of the NLP and SOCP models obtained with the simulation of IEEE 57-bus are presented graphically in Fig. 3, where it is highlighted the weightings with lower values of Ψ. The results obtained show that the lowest values of Ψ of the NLP model for Cases E1 and E2 occurred with the weights (0.3, 0.3, 0.4) and (0.2, 0.2, 0.6), respectively. On another hand, the results of the SOCP model show that the lowest values of Ψ for Cases E1 and E2 occurred with weights (0.4, 0.4, 0.2) and (0.3, 0.3, 0.4), respectively. Both the lower values of the NLP and SOCP models are similar for the case studies, then, the analysis of both models will be similar.

TABLE II
Mean and probability demand levels

IEEE 57-bus	b_1	b_2	b_3	b_4
π_b^D	1.0203	0.9837	0.9405	0.8240
	1.0032	0.9692	0.9022	0.8073
	0.9947	0.9561	0.8495	0.7811
ρ_b^D	0.30	0.30	0.30	0.30
	0.40	0.40	0.40	0.40
	0.30	0.30	0.30	0.30

TABLE III
Case E1 results – IEEE 57-bus system

Model	$\sigma_1, \sigma_2, \sigma_3$	F_1[US$10^7]	F_2[US$10^7]	F_3[kTon]	Time[s]
NLP	1.0, 0.0, 0.0	30.01	5.54	40.46	6
	0.0, 1.0, 0.0	32.05	1.27	23.94	4
	0.2, 0.2, 0.6	30.80	1.56	22.84	4
	0.0, 0.0, 1.0	31.07	1.37	22.45	37
SOCP	1.0, 0.0, 0.0	30.00	5.55	40.58	30
	0.0, 1.0, 0.0	32.05	1.26	23.94	25
	0.3, 0.3, 0.4	30.78	1.56	22.87	25
	0.0, 0.0, 1.0	31.07	1.36	22.45	18

TABLE IV
Case E2 results – IEEE 57-bus system

Model	$\sigma_1, \sigma_2, \sigma_3$	F_1[US$10^7]	F_2[US$10^7]	F_3[kTon]	Time[s]
NLP	1.0, 0.0, 0.0	26.30	2.07	0.36	7
	0.0, 1.0, 0.0	27.01	1.43	0.28	4
	0.2, 0.2, 0.6	26.52	1.69	0.29	4
	0.0, 0.0, 1.0	26.99	1.97	0.26	53
SOCP	1.0, 0.0, 0.0	26.30	2.05	0.36	28
	0.0, 1.0, 0.0	27.00	1.42	0.28	23
	0.3, 0.3, 0.4	26.51	1.68	0.30	28
	0.0, 0.0, 1.0	27.85	5.84	0.26	9

Taking Case E1 as a reference, when the power system combines RES and non-RES (Case E2), it appears that the values of F_1 (energy generation cost) and F_3 (emission of polluting gases) are reduced, while in some cases an increase in of F_2 (active power loss) is observed. The reduction in F_1 and F_3 is due to the lower energy generation costs and the absence of pollutant emissions in the environment of the WGs and PVs in comparison with TGs. The increase in F_2 in some weights is a consequence of the dependence of the climatic conditions of the WGs and PVs to generate energy. In this way, other generation types must produce energy to meet demand.

In Case E2, with a weight of $\sigma_3 = 1$, the SOCP model presents a higher F_2 value when compared to the NLP model owing to two factors: (i) The RES was not installed optimally in the system because, in this study, the TG generations with less generation capacity and higher connected loads were replaced; and, (ii) Because of relaxation (27), the SOCP model is unable to find the optimal point of operation, which was found by the NLP model.

The conflicting behavior between the functions F_1 and F_2 in all cases analyzed of the NLP and SOCP models is presented in Fig. 3. Because of the high penetration of RES

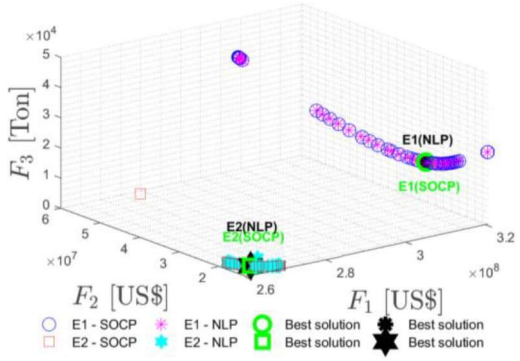

Fig. 3 - Pareto frontiers - IEEE 57-bus system

TABLE V
Mean and probability demand levels

IEEE 118-bus	b_1	b_2	b_3	b_4
π_b^D	1.0979	1.0106	0.9271	0.7962
	1.0542	0.9783	0.8884	0.7717
	1.0346	0.9528	0.8362	0.7211
ρ_b^D	0.30	0.30	0.30	0.30
	0.40	0.40	0.40	0.40
	0.30	0.30	0.30	0.30

TABLE VI
Case E1 results – IEEE 118-bus system

Model	$\sigma_1, \sigma_2, \sigma_3$	F_1[US$10^7]	F_2[US$10^7]	F_3[kTon]	Time[s]
NLP	1.0, 0.0, 0.0	77.19	11.65	98.03	36
	0.0, 1.0, 0.0	93.91	8.14	67.15	40
	0.3, 0.3, 0.4	77.42	10.98	97.86	44
	0.0, 0.0, 1.0	94.18	8.83	56.74	83
SOCP	1.0, 0.0, 0.0	77.19	11.65	98.03	143
	0.0, 1.0, 0.0	93.73	7.27	66.80	108
	0.5, 0.5, 0.0	77.41	11.97	97.89	124
	0.0, 0.0, 1.0	94.18	8.83	56.74	79

TABLE VII
Case E2 results – IEEE 118-bus system

Model	$\sigma_1, \sigma_2, \sigma_3$	F_1[US$10^7]	F_2[US$10^7]	F_3[kTon]	Time[s]
NLP	1.0, 0.0, 0.0	59.94	11.90	38.28	42
	0.0, 1.0, 0.0	87.17	6.48	42.80	44
	0.3, 0.3, 0.4	60.39	10.81	38.55	31
	0.0, 0.0, 1.0	77.10	10.54	23.42	134
SOCP	1.0, 0.0, 0.0	59.93	11.88	38.27	164
	0.0, 1.0, 0.0	87.08	5.85	42.26	129
	0.2, 0.2, 0.6	60.39	10.80	38.55	141
	0.0, 0.0, 1.0	76.65	10.50	23.43	84

in the system, it is noted that the results presented in Case E2 for both models are considerably different from those of Case E1. The objective functions F_1 and F_3 present conflicting behavior in Cases E1 and E2 for both models. In Cases E1 and E2 for both models, the objective functions F_3 and F_2 are not in conflict owing to both the high concentration of the RES and the system configuration. In this way, if the operator of the electrical system knows that information, it will be able to make better quality strategic decisions based on the results of developed simulations.

B. IEEE 118-bus system

The IEEE 118-bus is a medium-sized system with a high reactive capacity that presents considerable computational complexity for simulating stochastic models. For Case E1, all the generation units are TG. For Case E2, buses 4, 24, 26, 31, 40, 42, and 69, are HG units; buses 1, 15, 19, and 56 are WG buses 73, 91, 99, and 107 are PV; and the remainder of the generation units are TG. TABLE V shows the average demand levels for each operational scenario.

The extreme points of the Pareto front and the minimum values of the objective function Ψ for Cases E1 and E2 are presented in TABLE VI and TABLE VII, respectively. The results of the NLP and SOCP models are shown in Fig. 4 for

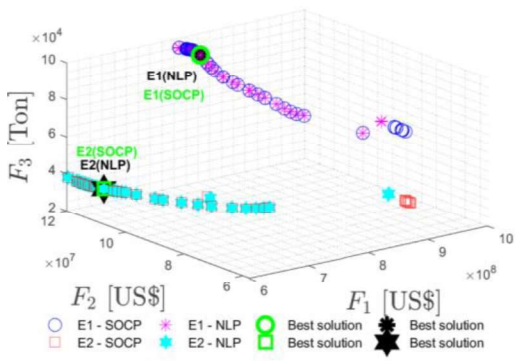

Fig. 4- Pareto frontiers – IEEE 118-bus system

Cases E1 and E2, highlighting the weightings with the minimum values of Ψ. The solution of the NLP model presents the minimum value with the weigh combination (0.3, 0.3, 0.4) for Cases E1 and E2. On the other hand, the solution of the SOCP model presents the minimum objective function values with the weight combinations (0.5, 0.5, 0.0) and (0.2, 0.2, 0.6), for Cases E1 and E2, respectively.

Considering Case E1 as a reference, when the system combines RES and non-RES, F_1 and F_3 decrease thanks to lower energy generation costs and non-emission of pollutants from WGs and PVs, and an increase in some values of F_2 results from the climate dependence of the WGs and PVs in electricity generation (non-dispatchable sources). Thus, TG and HG sources must supply the demand when RESs are not producing energy.

The results presented by the NLP and SOCP models in both Cases E1 and E2 were similar. However, the extreme points with weight $\sigma_2 = 1$ for both cases present the greatest difference between the results of models, approximately 11%, due to the absence of a previous study of optimal RES allocation in the system and the imprecision caused by the relaxation (27).

The conflicting behavior between the functions F_1 and F_2 in all cases analyzed of the NLP and SOCP models can be observed in Fig. 4. The functions F_1 and F_3 in Case E1 present conflicting behavior for both models. The functions F_3 and F_2 present conflicting behavior only in Case E2 and NLP and SOCP models, unlike Case E1, because of the absence of RES in the network. In Case E2, F_1 and F_3 do not present conflicting behavior, owing to the network configuration and the climatic dependence of RES (non-dispatchable sources).

IV. Conclusion

This paper presented a multi-objective second-order conic programming model to solve the optimal power dispatch in power systems regarding the inclusion of renewable energy sources. Uncertainties were considered through a stochastic scenario-based approach to duly represent the behavior of RES and load of the system. The objective functions: cost of electricity generation, cost of active loss, and the emission of polluting gases from non-RES, present conflicting and non-conflicting behaviors depending on the location, concentration, climatic dependence of RES in the power system, and the network configuration. Thus, these objective functions were satisfactorily combined into a single objective function through a weighted approach to obtain a Pareto front for the problem.

Results showed that by changing the energy matrix of a system with the installation of RES, the emission of pollutants and generation costs of the system are reduced, but the values of active losses of the network increase because of RES allocation problems and climatic dependence of WG and PV generation allocation (non-dispatchable sources). This problem could be mitigated through an initial study of the optimized allocation of RES in the EPS.

Numerical experiments revealed that the SOCP model presents some deviations in the objective function value when compared with the solutions obtained with the exact NLP model. The consideration of the minimum resistance in the branches improve the convexity of the SOCP model; however, a more detailed analysis of the solution is necessary. Future works can compare not only the objective function value but also the active and reactive power dispatches.

References

[1] A. Gómez-Expósito, A. J. Conejo, and C. Cañizares, Electric energy systems: Analysis and operation, vol. 17. CRC Press, 2017.

[2] D. K. Molzahn and I. A. Hiskens, "A survey of relaxations and approximations of the power flow equations," Found. Trends® Electr. Energy Syst., vol. 4, no. 1–2, pp. 1–221, 2019, doi: 10.1561/3100000012.

[3] J. E. Oliver, "Kyoto protocol," in Encyclopedia of World Climatology, vol. 10, no. 1, Springer Netherlands, 2007, pp. 443–443.

[4] C. L. Spash, "The brave new world of carbon trading," New Polit. Econ., vol. 15, no. 2, pp. 169–195, Jun. 2010, doi: 10.1080/13563460903556049.

[5] A. Alqurashi, A. H. Etemadi, and A. Khodaei, "Treatment of uncertainty for next generation power systems: State-of-the-art in stochastic optimization," Electr. Power Syst. Res., vol. 141, pp. 233–245, Dec. 2016, doi: 10.1016/j.epsr.2016.08.009.

[6] M. A. Abido, "Multiobjective evolutionary algorithms for electric power dispatch problem," IEEE Trans. Evol. Comput., vol. 10, no. 3, pp. 315–329, Jun. 2006, doi: 10.1109/TEVC.2005.857073.

[7] L. H. Wu, Y. N. Wang, X. F. Yuan, and S. W. Zhou, "Environmental/economic power dispatch problem using multi-objective differential evolution algorithm," Electr. Power Syst. Res., vol. 80, no. 9, pp. 1171–1181, Sep. 2010, doi: 10.1016/j.epsr.2010.03.010.

[8] F. Chen, G. H. Huang, Y. R. Fan, and R. F. Liao, "A nonlinear fractional programming approach for environmental-economic power dispatch," Int. J. Electr. Power Energy Syst., vol. 78, pp. 463–469, 2016, doi: 10.1016/j.ijepes.2015.11.118.

[9] E. X. S. Araujo, M. C. Cerbantes, and J. R. S. Mantovani, "Optimal power flow with renewable generation: a modified NSGA-II-based probabilistic solution approach," J. Control. Autom. Electr. Syst., no. March 2015, May 2020, doi: 10.1007/s40313-020-00596-7.

[10] S. Shargh, B. Khorshid ghazani, B. Mohammadi-ivatloo, H. Seyedi, and M. Abapour, "Probabilistic multi-objective optimal power flow considering correlated wind power and load uncertainties," Renew. Energy, vol. 94, pp. 10–21, Aug. 2016, doi: 10.1016/j.renene.2016.02.064.

[11] L. Baringo and A. J. Conejo, "Correlated wind-power production and electric load scenarios for investment decisions," Appl. Energy, vol. 101, pp. 475–482, Jan. 2013, doi: 10.1016/j.apenergy.2012.06.002.

[12] J. Qiu, J. Zhao, Y. Zheng, Z. Dong, and Z. Y. Dong, "Optimal allocation of BESS and MT in a microgrid," IET Gener. Transm. Distrib., vol. 12, no. 9, pp. 1988–1997, May 2018, doi: 10.1049/iet-gtd.2017.0717.

[13] C. Zhang, Q. Wang, Y. Ding, and J. Ostergaard, "A multi-objective model for transmission planning under uncertainties," in 2014 IEEE Electrical Power and Energy Conference, Nov. 2014, pp. 42–47, doi: 10.1109/EPEC.2014.8.

[14] R. Fourer, D. M. Gay, and B. W. Kernighan, A modeling language for mathematical programming. 1990.

[15] S. Babaeinejadsarookolaee et al., "The power grid library for benchmarking ac optimal power flow algorithms," arXiv, pp. 1–17, Aug. 2019, [Online]. Available: http://arxiv.org/abs/1908.02788.

[16] Brazilian Electricity Commercialization Chamber, "No 022 – 27o leilão de energia nova (A-4)," 2019. https://www.ccee.org.br/ccee/documentos/CCEE_640187 (accessed May 23, 2019).

[17] C. Josz and D. K. Molzahn, "Lasserre hierarchy for large scale polynomial optimization in real and complex variables," SIAM J. Optim., vol. 28, no. 2, pp. 1017–1048, Jan. 2018, doi: 10.1137/15M1034386.

[18] D. K. Molzahn, J. T. Holzer, B. C. Lesieutre, and C. L. DeMarco, "Implementation of a large-scale optimal power flow solver based on semidefinite programming," IEEE Trans. Power Syst., 2013, doi: 10.1109/TPWRS.2013.2258044.

[19] C. de C. de E. E. (CCEE), "Preço médio mensal MWh/Average monthly price MWh," 2021. https://www.ccee.org.br/portal/faces/pages_publico/o-que-fazemos/como_ccee_atua/precos/preco_media_mensal (accessed Jul. 01, 2021).

[20] I. Staffell and S. Pfenninger, "Renewables.ninja," 2015. https://www.renewables.ninja/.